



Published in final edited form as:

Nat Cell Biol. 2017 November ; 19(11): 1326–1335. doi:10.1038/ncb3632.

Synthetic Hydrogels for Human Intestinal Organoid Generation and Colonic Wound Repair

Ricardo Cruz-Acuña^{1,3,*}, Miguel Quirós^{4,*}, Attila E. Farkas⁵, Priya H. Dedhia^{6,7,8}, Sha Huang^{6,7,8}, Dorothée Siuda⁴, Vicky García-Hernández⁴, Alyssa J. Miller⁶, Jason R. Spence^{6,7,8,#}, Asma Nusrat^{4,#}, and Andrés J. García^{2,3,#}

¹Wallace H. Coulter Department of Biomedical Engineering, Georgia Institute of Technology, Atlanta, GA 30332

²George W. Woodruff School of Mechanical Engineering, Georgia Institute of Technology, Atlanta, GA 30332

³Parker H. Petit Institute for Bioengineering and Biosciences, Georgia Institute of Technology, Atlanta, GA 30332

⁴Department of Pathology, University of Michigan, Ann Arbor, MI, 48104

⁵Biological Research Centre, Hungarian Academy of Sciences, Szeged, Hungary, 6726

⁶Department of Internal Medicine, Division of Gastroenterology, University of Michigan Medical School, Ann Arbor, MI, 48104

⁷Department of Cell and Developmental Biology, University of Michigan Medical School, Ann Arbor, MI, 48104

⁸Center for Organogenesis, University of Michigan Medical School, Ann Arbor, MI, 48104

Abstract

In vitro differentiation of human intestinal organoids (HIOs) from pluripotent stem cells is an unparalleled system for creating complex, multi-cellular 3D structures capable of giving rise to tissue analogous to native human tissue. Current methods for generating HIOs rely on growth in an undefined tumor-derived extracellular matrix (ECM), which severely limits use of organoid technologies for regenerative and translational medicine. Here, we developed a fully defined, synthetic hydrogel based on a four-armed, maleimide-terminated poly(ethylene glycol) macromer that supports robust and highly reproducible *in vitro* growth and expansion of HIOs such that 3D

Users may view, print, copy, and download text and data-mine the content in such documents, for the purposes of academic research, subject always to the full Conditions of use: http://www.nature.com/authors/editorial_policies/license.html#terms

Co-last authors and to whom correspondence should be addressed: A.J. García (andres.garcia@me.gatech.edu), A. Nusrat (anusrat@med.umich.edu), J.R. Spence (spencejr@umich.edu).

*These first authors contributed equally to this work.

#These last authors contributed equally to this work.

Author contributions: R.C.A. and M.Q. conducted all experiments, collected data and performed data analyses. A.E.F. assisted with *in vitro* and *in vivo* intestinal crypt experiments. P.H.D. performed the *in vivo* HIO implantation under kidney capsule experiment. S.H. performed the culture and differentiation of PSCs into intestinal spheroids. D.S. assisted with *in vivo* HIO delivery to mouse colonic wounds. V.G.H. and A.M. performed the *in situ* hybridization experiments. A.N., A.J.G., and J.R.S. conceptualized and designed the project and experiments. R.C.A., A.J.G., A.N., J.R.S., and M.Q. wrote the manuscript.

The authors declare no competing financial interests.

structures are never embedded in tumor-derived ECM. We also demonstrate that the hydrogel serves as an injectable HIO vehicle that can be delivered into injured intestinal mucosa resulting in HIO engraftment and improved colonic wound repair. Together, these studies show proof-of-concept that HIOs may be used therapeutically to treat intestinal injury.

Human pluripotent stem cells (hPSCs), such as embryonic stem cells (ESCs)¹ and induced pluripotent stem cells (iPSCs)², are important cell sources for regenerative therapies and modeling of human diseases³⁻⁵. *In vitro* generation of human organoids from hPSCs offers unparalleled strategies for generating multi-cellular 3D structures recapitulating important features of epithelial and mesenchymal tissues⁶⁻⁹. For example, human intestinal organoid (HIO) technology provides a powerful platform for functional modeling and repair of genetic defects in human intestinal development^{10,11} and the establishment of chronic disease models, such as inflammatory bowel disease¹².

In order to generate HIOs, hPSCs are cultured and differentiated using growth factors in a MatrigelTM-coated substrate, giving rise to 3D intestinal spheroids which are collected and encapsulated within MatrigelTM for expansion into HIOs¹³. MatrigelTM is a heterogeneous, complex mixture of ECM proteins, proteoglycans, and growth factors secreted by Engelbreth-Holm-Swarm mouse sarcoma cells¹⁴, which is required for 3D growth and expansion of HIOs. However, MatrigelTM suffers from lot-to-lot compositional and structural variability and, importantly, this tumor-derived matrix has limited clinical translational potential¹⁵. Indeed, a synthetic alternative to MatrigelTM that supports murine intestinal stem cell expansion and organoid formation has been recently reported¹⁵.

Here, we describe a completely synthetic hydrogel that supports *in vitro* generation of intestinal organoids from human ESC- and iPSC-derived 3D spheroids without MatrigelTM encapsulation and promotes their engraftment and healing of murine colonic mucosal wounds. Hydrogel mechanical properties and adhesive ligand type were key parameters in engineering a synthetic ECM mimic that supported HIO viability, expansion and development. Additionally, this synthetic hydrogel served as an injectable vehicle to deliver HIOs to intestinal wounds via a colonoscope resulting in organoid survival, engraftment, and wound repair. The modular design of this synthetic matrix and ability to deliver via endoscopic techniques support the translational potential of this delivery platform for regenerative medicine and overcomes limitations associated with the use of MatrigelTM for hPSC-based organoid technologies.

Engineered hydrogels support HIO viability

We selected a hydrogel platform based on a four-arm poly(ethylene glycol) (PEG) macromer with maleimide groups at each terminus (PEG-4MAL) (Supplementary Fig. 1a), which exhibits high cytocompatibility and minimal toxicity and inflammation *in vivo*^{16,17}. Moreover, this hydrogel system offers significant advantages due to its well-defined structure, stoichiometric incorporation of biofunctional groups, and tunable reaction time scales for *in situ* gelation for *in vivo* applications^{16,17}.

PEG-4MAL macromers were functionalized with adhesive peptides and crosslinked in the presence of cells to generate PEG-4MAL hydrogels (Supplementary Fig. 1a,b). The mechanical properties of the hydrogel were tuned by varying polymer density (Supplementary Fig. 1c,d). We explored hydrogel formulations that supported the viability of ESC-derived HIOs that were first generated in Matrigel™. After HIOs were grown in Matrigel™, they were retrieved and encapsulated in PEG-4MAL hydrogel formulations (Supplementary Fig. 1e). Because ECM mechanical properties influence epithelial cell behaviors¹⁸, we investigated the influence of hydrogel polymer density (3.5-6.0% wt/vol), which controls hydrogel mechanical properties (Supplementary Fig. 1c,d), on HIO viability at day 7 post-encapsulation (Fig. 1a). For reference, the mechanical properties of Matrigel™ ($G' = 78$ Pa, $G'' = 5.8$ Pa) are in the range of the 3.5-4.0% PEG-4MAL formulations. These synthetic hydrogels were engineered to present a constant 2.0 mM RGD adhesive peptide (GRGDSPC) density and crosslinked with the protease-degradable peptide GPQ-W (GCRDGPQGIWGQDRCG). This adhesive peptide type and density were chosen as they have been shown to support high epithelial cell viability and cyst formation in PEG-4MAL hydrogels¹⁸. The protease-degradable crosslinking peptide is necessary for cell-dependent matrix remodeling, cell migration and growth^{18,19}. HIOs embedded in 3.5% and 4.0% PEG-4MAL gels grew as cysts with an epithelium and central lumen, and maintained high viability for at least 7 d in culture comparable with growth and viability of HIOs in Matrigel™ (Fig. 1a). Quantification of organoid viability area demonstrated no significant differences between HIOs embedded in 3.5% or 4.0% PEG-4MAL gels and HIOs in Matrigel™ (Fig. 1b). In contrast, organoids encapsulated in 5.0% or 6.0% PEG-4MAL hydrogels exhibited significantly reduced viability at day 7 after encapsulation as compared to HIOs embedded in 3.5%, 4.0% PEG-4MAL gels or Matrigel™ (Fig. 1a,b). These results suggest polymer density-dependent effects on HIO survival within PEG-4MAL hydrogels. Although 3.5% PEG-4MAL hydrogels supported high HIO viability, this formulation was less mechanically stable compared to 4.0% PEG-4MAL hydrogels by 7 days in culture. We therefore selected 4.0% PEG-MAL hydrogels for subsequent studies.

Interactions between adhesion receptors and ECM provide signals critical for cell survival, proliferation and differentiation²⁰. Therefore, we examined whether the adhesive ligand type in the synthetic hydrogel impacts HIO viability. Organoids were embedded within PEG-4MAL formulations of 4.0% polymer density and constant GPQ-W crosslinking peptide density but with different cysteine-terminated adhesive peptides (all at 2.0 mM; Fig. 1c,d): RGD, laminin α 1 chain-derived AG73 (CGGRKRLQVQLSIRT)²¹, type I collagen-mimetic triple helical GFOGER (GYGGGP(GPP)₅GFOGER(GPP)₅GPC)²², and laminin α 1 chain-derived IKVAV (CGGAASIKVAVSADR)²³. Because the adhesive peptide-functionalized macromer building blocks of the hydrogel are symmetric and form a regular mesh structure that is fully swollen, the adhesive peptide is uniformly distributed throughout the hydrogel network within the 'statistical average' of the mesh size (30-40 nm). Furthermore, because of the small size of the PEG macromer arms and the swollen state of the gel, the mobility of the adhesive peptide is very limited and there is no effective clustering of the adhesive peptide¹⁸. Nevertheless, changes in adhesive peptide density at the nanoscale cannot be completely ruled out. Organoids encapsulated in RGD-functionalized hydrogels maintained high viability for at least 7 d after encapsulation (Fig. 1c,d; Fig. 2a),

similar to viability within Matrigel™. In contrast, organoids encapsulated in PEG-4MAL hydrogels functionalized with AG73, GFOGER or IKVAV showed reduced viability at 7 d post-encapsulation (Fig. 1c,d). Adhesion to RGD was required for HIO viability as organoids encapsulated in hydrogels presenting an inactive scrambled peptide (RDG) showed reduced viability at 7 d post-encapsulation (Fig. 2b). Finally, organoids exhibited low viability at 7 d post-encapsulation in hydrogels crosslinked with non-degradable molecules (DTT, Fig. 2c), demonstrating that prolonged survival of HIO requires a degradable matrix. Taken together, these results identify an engineered hydrogel formulation (4.0% polymer density, 2.0 mM RGD adhesive peptide, GPQ-W crosslinking peptide) that supports high viability for established HIOs, and which was used for all subsequent experiments.

Engineered hydrogel supports HIO development

We next examined HIO maintenance during culture in engineered hydrogels. Over several days in culture, established HIOs grew in size, changed shape, maintained a central lumen, and displayed epithelial budding at the interface with the hydrogel (Fig. 2d). Additionally, mesenchymal cells were observed migrating into the hydrogel, similar to HIOs maintained in Matrigel™ (Fig. 2d,e). To further characterize the intestinal epithelium of HIOs, we examined cell proliferation and apicobasal polarity in HIOs generated in Matrigel™ and those transferred to the engineered PEG-4MAL hydrogels. After 7 d in culture, HIOs stained positive for KI67, indicating cell proliferation, demonstrated appropriate polarization of apical (EZRIN) and basolateral (β -CATENIN) proteins, and localization of an epithelial tight junction protein (ZO-1)²⁴ (Fig. 2f,g). The staining patterns were similar when comparing HIOs maintained in PEG-4MAL hydrogel and Matrigel™ (Fig. 2f,g), demonstrating that the engineered PEG-4MAL hydrogel robustly supports HIO maintenance.

Engineered hydrogel generates HIOs from spheroids

The use of Matrigel™ to generate HIOs is a fundamental roadblock to the clinical translation of organoid technologies. We therefore examined whether the engineered PEG-4MAL hydrogel supports survival of hESC-derived intestinal spheroids and growth into HIOs without ever embedding in Matrigel™. After 4-5 days of induction towards the intestinal lineage on a Matrigel™-coated substrate, small 3D intestinal spheroids self-assemble and bud off from the cultured monolayer losing contact with Matrigel™. Detached, floating mCherry-expressing intestinal spheroids were collected from the media and encapsulated in PEG-4MAL hydrogels formulated over a range of polymer densities (3.5%-12.0%) (Supplementary Fig. 1f) to examine a range of mechanical properties (Supplementary Fig. 1c,d). All these hydrogels were engineered to present 2.0 mM RGD adhesive peptide and crosslinked with GPQ-W. Spheroids embedded in 3.5% and 4.0% PEG-4MAL maintained viability at 2 h after encapsulation and grew into larger structures reminiscent of organoids with high viability at 5 d after encapsulation (Fig. 3a). In contrast, spheroids encapsulated in 8.0% and 12.0% PEG-4MAL hydrogels displayed significantly lower viability at 2 h post-encapsulation when compared to spheroids embedded in 3.5% or 4.0% PEG-4MAL (Fig. 3a). Consistent results were observed between hESC- and hiPSC-

derived spheroids (Supplementary Fig. 2). hiPSC-derived intestinal spheroids encapsulated in 4.0% PEG-4MAL grew into organoids with high viability at 5 d after encapsulation and developed over 3 weeks into HIOs similar to spheroids encapsulated in Matrigel™ (Supplementary Fig. 2a,b). In contrast, hiPSC-derived spheroids encapsulated in 8.0% PEG-4MAL hydrogels showed very low viability by 1 d post-encapsulation (Supplementary Fig. 2c).

The strong dependence of spheroid and HIO viability on hydrogel polymer density suggests that the mechanical properties of these synthetic matrices regulate organoid survival. However, varying polymer density also alters the mesh size for these networks, which can impact diffusional properties of the hydrogel. It is not possible to uncouple mechanical properties from diffusional properties over the full range of polymer densities (3.5%-12.0%) examined in this study. However, we compared organoid viability and size in RGD-functionalized hydrogels from different macromer sizes (20 vs. 40 kDa) but different polymer densities (4.0% vs. 8.0%) and engineered to have equivalent crosslinking densities (Supplementary Fig. 3a-c). These hydrogels exhibit different diffusive characteristics/permeability caused by the differences in macromer arm length but have equivalent mechanical properties due to equivalent crosslinking densities¹⁸. ESC-derived spheroids developed normally into HIOs after 5 days of encapsulation in either hydrogel formulation showing no differences in HIO viability (Supplementary Fig. 3a,b), and no differences in projected area and longest distance between two points along the projected area (Feret diameter; Supplementary Fig. 3c). These results suggest that polymer density-dependent spheroid survival and development into HIOs is related to hydrogel mechanical properties. Furthermore, we evaluated the role of known mechanotransduction pathways on spheroid survival. Inhibition of nuclear translocation of yes-associated protein (YAP), which has been implicated in mechanotransduction and regulation of intestinal stem cell self-renewal¹⁵, using verteporfin resulted in significant cell death for spheroids encapsulated in PEG-4MAL hydrogels compared to vehicle control (Supplementary Fig. 3d-f). Treatment with blebbistatin or Y-27632, which inhibit myosin II and Rho-associated kinase^{25,26}, respectively, resulted in dose-dependent increases in apoptosis and spheroid death at 1 d post-encapsulation (Supplementary Fig. 3d-f). These results provide a preliminary indication that YAP and cellular contractility are important in the initial stages of human intestinal spheroid survival and development into HIOs.

We next analyzed HIO generation from ESC-derived spheroids cultured within the engineered synthetic matrix (4.0% polymer density, 2.0 mM RGD, GPQ-W crosslinker). Intestinal spheroids cultured within PEG-4MAL hydrogels grew in size over 7 d as shown by a 2-fold increase in projected area (Fig. 3b) and 1.4-fold increase in Feret diameter (Fig. 3c) as compared to the day of encapsulation (Day 0; Fig. 3b,c). There were no differences in spheroid area, diameter, or growth rates between spheroids cultured in PEG-4MAL hydrogels and Matrigel™ (Fig. 3b,c). Similar to our observations for established HIOs, spheroids changed shape during expansion and displayed epithelial budding at the interface with the hydrogel and cell outgrowths migrating into the hydrogel (Supplementary Fig. 2d). During HIO development, spheroids cultured in PEG-4MAL hydrogels were passaged in a similar manner as previously described for Matrigel^{13,27}. Immunostaining analyses at 21 d post-encapsulation demonstrated that organoids generated in engineered PEG-4MAL

hydrogels were proliferating as shown by KI67 labeling, had polarized distribution of apical EZRIN and basolateral β -CATENIN, and expressed ZO-1 in the apical junctional complex (Fig. 3d,e). These staining patterns were identical to organoids generated in Matrigel™. Quantitative reverse transcription polymerase chain reaction (RT-qPCR) confirmed that expression levels of pluripotency (OCT4), endoderm (FOXA2), and epithelial junction (ZO1, ECAD and CLDN2) markers in hydrogel-encapsulated spheroids were comparable to those embedded in Matrigel™ and had similar behaviors during early timepoints while developing into HIOs (Supplementary Fig. 4). Finally, to test whether these synthetic matrices are suitable for the culture of other human organoids, we embedded human lung organoids (HLOs)^{28,29} in engineered PEG-4MAL hydrogels (Supplementary Fig. 5). HLOs cultured in PEG-4MAL hydrogels maintained high viability 7 d after encapsulation (Supplementary Fig. 5a), and demonstrated an organized lung epithelium (ECAD), lumen formation, and specific markers for lung epithelium (NKX2.1) and airway basal cells (P63) as assessed by immunostaining analyses (Supplementary Fig. 5b)^{28,29}. Taken together, these results demonstrate that this fully synthetic hydrogel supports the generation of ESC- and iPSC-derived HIOs from the intestinal spheroid stage without the use of Matrigel™, and has the potential to be adapted for the generation of different human organoids.

Hydrogel-generated HIOs differentiate in vivo

We next examined the potential of hydrogel-grown HIOs to differentiate into mature intestinal tissue *in vivo* as previously demonstrated^{24,30}. mCherry-expressing spheroids that were embedded and grown within engineered PEG-4MAL hydrogels or in Matrigel™ for 3 weeks were recovered from their respective matrix and implanted under the kidney capsule of immunocompromised NSG mice (Fig. 4). In addition, HIOs grown in Matrigel™ for 2 weeks and then transferred and cultured within PEG-4MAL hydrogels for 1 week (hydrogel-maintained) were implanted under the kidney capsule (Fig. 4a,b,d). After 12 weeks, implanted kidneys contained mCherry-expressing HIOs that were 10- to 40-fold larger in area than at the time of implantation (Fig. 4a,b), consistent with previous reports. Dissected PEG-4MAL-generated HIOs showed differentiated intestinal epithelium that resembled mature human intestine with crypt-villus architecture and underlying lamina propria, muscularis mucosae and submucosa²⁴, with structured collagen fibers (trichrome) and presence of differentiated goblet cells (alcian blue), comparable to Matrigel™-generated and hydrogel-maintained organoids (Fig. 4c,d). Polarized epithelial differentiation of PEG-4MAL hydrogel-generated HIOs was demonstrated by immunostaining for β -CATENIN, EZRIN, ZO-1 and ECAD (Fig. 5a). Additionally, PEG-4MAL-generated organoid epithelium showed localized cell proliferation (KI67) at the base of the crypt where the intestinal stem cells reside, and expressed characteristic markers for the intestinal epithelial protein CDX2, enteroendocrine cells (CHGA), goblet cells (MUC2), and tuft cells (DCLK1)³¹. Furthermore, PEG-4MAL-generated HIOs expressed PDX1, demonstrating a duodenum regional identity (Fig. 5a)¹³. Expression was comparable to Matrigel™-generated organoids and hydrogel-maintained organoids (Fig. 5b). These results demonstrate that HIOs generated in the engineered synthetic matrix can differentiate into mature intestinal tissue in an *in vivo* environment to the same extent as HIOs generated within Matrigel™. These

findings establish engineered synthetic PEG-4MAL hydrogels as a robust alternative to Matrigel™ with significant implications for translational medicine.

Hydrogels as a HIO delivery vehicle to heal colonic wounds

A key advantage of the PEG-4MAL hydrogel system is control over gelling time so that the hydrogel components can be injected as a solution that gels *in situ*¹⁷. We therefore explored the use of the engineered hydrogel as a delivery vehicle for HIOs into murine intestinal mucosal wounds using a murine colonoscope. HIOs generated in PEG-4MAL hydrogels or Matrigel™ were recovered from their matrix, mixed with the hydrogel precursor solution, and injected at the site of mechanically-induced mucosal wounds in the distal colon of immunocompromised mice (Fig. 6a, Supplementary Fig. 6a)³². Wound closure was evaluated using a colonoscope, and fluorescence imaging showed localized expression of mCherry-positive tissue at the wound site 5 d post-injection (Fig. 6b). Immunostaining at 4 weeks post-injection demonstrated that HIO delivery via the synthetic hydrogel resulted in HIO engraftment into host intestinal epithelial tissue as shown by positive staining for human nuclei (NUMA) to detect either HIOs generated in the PEG-4MAL hydrogel or Matrigel™ (Fig. 6c). Importantly, no staining was evident for no-injection control, only hydrogel, and HIOs injected in saline (Fig. 6c), demonstrating that the hydrogel delivery vehicle is required for HIO engraftment and wound repair. Examination of HIO engraftment at the wound edge demonstrated staining for human cells adjacent to host tissue which stained negative for human markers. Engraftment of human cells into the colonic wound was also confirmed by positive staining for human mitochondria (HUMIT; Supplementary Fig. 6b). Furthermore, colonic wounds treated with HIOs delivered with hydrogel showed positive staining for an *OLFM4* probe specific to human cells at the base of the crypt-like domain (Fig. 6d; Supplementary Fig. 6c), a pattern consistent with staining in the normal adult human colon (Supplementary Fig. 6c), which is also consistent with previous reports of human *OLFM4* protein and/or mRNA localization³³⁻³⁵. Additionally, several negatively stained human crypt-like domains were adjacent to mouse intestinal crypts which stained positive for a mouse-specific *Lgr5* probe (Supplementary Fig. 6d) via *in situ* hybridization³⁶. These observations were compared to control tissue sections from immunocompromised mice that did not undergo colonic injuries or received HIO injections (Fig. 6d; Supplementary Fig. 6d).

We also examined whether delivered HIOs promote colonic mucosal wound repair (Fig. 6e). Strikingly, delivery of HIOs to colonic wounds using the hydrogel carrier significantly increased wound closure compared to untreated wounds and wounds treated with hydrogel alone or HIOs without the hydrogel carrier (Fig. 6e). No differences were observed in wound closure between HIOs generated in the synthetic hydrogels and Matrigel™. Taken together, these results demonstrate that the engineered PEG-4MAL hydrogel serves as an injectable delivery vehicle that supports localized HIO engraftment in colonic mucosal wounds and enhances wound closure. These findings establish the clinical translational potential of the synthetic hydrogel as an *in vivo* delivery vehicle for hPSC-derived HIOs and provide proof-of-concept that HIOs may be used therapeutically to treat intestinal injury or disease.

In this study, we engineered a completely synthetic hydrogel that supports *in vitro* generation of intestinal organoids from hPSC-derived spheroids without the need of Matrigel™ encapsulation. Both mechanical and biochemical properties of the synthetic ECM were important to intestinal organoid formation, and we identified an optimal formulation that supports intestinal spheroid survival, expansion and epithelial differentiation into HIOs and differentiation into mature intestinal tissue *in vivo* to similar levels as Matrigel™. Additionally, we showed that this synthetic matrix supports the development of other human organoids such as HLOs. The requirement for specific mechanical and cell adhesive properties in the synthetic matrix is consistent with previous work showing that epithelial cell cyst growth, polarization, and lumen formation are restricted to a narrow range of ECM elasticity and that adhesive peptide type regulates apicobasal polarity and lumenogenesis during epithelial morphogenesis in 3D cultures¹⁸. Interestingly, the mechanical properties and protease degradation characteristics that supported hPSC-derived organoids in this study are different from those recently identified for murine *Lgr5*⁺ intestinal stem cell growth and organoid formation¹⁵, which involved more complex, mechanically dynamic properties, and suggest differences between these two organoid sources. This fully synthetic matrix addresses major limitations of Matrigel™ associated with lot-to-lot compositional and structural variability and its tumor-derived nature that severely restrict scale-up applications and clinical translation.

We also established the use of the engineered hydrogel as a delivery vehicle for HIOs to murine intestinal mucosal wounds using a murine colonoscope. Although other studies have focused on the delivery of murine intestinal organoids into the colonic lumen as a suspension⁷, we showed that absence of a delivery vehicle reduces HIO engraftment at the implantation site. Injection of hydrogel liquid precursors and HIOs to mucosal wounds resulted in an *in situ* polymerized hydrogel that supported localized organoid engraftment and enhanced wound repair. Therefore, this delivery strategy forms a basis for the development of HIO-based therapies to treat gastrointestinal diseases in humans involving intestinal epithelial wounds (e.g., IBD). Furthermore, the modular nature of this hydrogel platform allows for the adaptation to *in vitro* generation and *in vivo* delivery of other human PSC-derived organoids (e.g., lung) for regenerative medicine.

Methods

Immunofluorescence analysis

For immunofluorescence labeling of frozen sections from colon, HIOs, kidney capsule implanted-HIOs or HLOs, these were fixed with 3.7% (w/v) paraformaldehyde at room temperature for 15 min, followed by 0.5% (w/v) Triton X-100 for 5 min. Primary antibody incubation was performed overnight at a 1:100 dilution, unless stated otherwise. Secondary antibody incubation was performed for 1 h at a 1:2000 dilution. Detailed information on the antibodies used including their resources (company names, catalogue numbers) and dilutions are provided in the Reporting Summary.

Differentiation of hPSCs into intestinal spheroids or HLOs

All work using human pluripotent stem cells was approved by the University of Michigan Human Pluripotent Stem Cell Oversight Committee (HPSCRO). Stem cell lines are routinely monitored for chromosomal karyotype, pluripotency (using a panel of antibody and RT-qPCR markers), and for the ability to undergo multi-lineage differentiation. For intestinal spheroid generation, mycoplasma-free human ES cells (H9, NIH registry #0062) and iPS cells (line 20.1, source as previously described¹³) were cultured on Matrigel™-coated plates and differentiated into intestinal tissue as previously described¹³. Floating spheroids present in the cultures on day 4 and day 5 of mid/hindgut induction were harvested for use in subsequent experiments. In some experiments, hESCs expressing a constitutively active H2BmCherry fluorescent reporter were used. This line was generated by infecting hESCs with a lentivirus containing PGK-H2BmCherry, which was a gift from Mark Mercola (Addgene plasmid # 21217)³⁷. For HLO generation, human ES cells (UM63-1, NIH registry #0277) were maintained, differentiated and expanded into HLOs as previously described²⁹.

Hydrogel formation and *in vitro* intestinal spheroid/HIO

To prepare PEG hydrogels, PEG-4MAL macromer (MW 22,000 or 44,000; Laysan Bio) was dissolved in 4-(2-hydroxyethyl)piperazine-1-ethanesulfonic acid (HEPES) buffer (20 mM in DPBS, pH 7.4). Adhesive and GPQ-W crosslinking peptides were custom synthesized by AAPPTec. Adhesive peptides RGD (GRGDSPC), AG73 (CGGRKRLQVQLSIRT), GFOGER (GYGGGP(GPP)₅GFOGER(GPP)₅GPC), IKVAV (CGGAASIKVAVSADR) and RDG (GRDGSPC) were dissolved in HEPES at 10.0 mM (5X final ligand density) and mixed with PEG-4MAL at a 2:1 PEG-4MAL/ligand ratio to generate functionalized PEG-4MAL precursor. Bis-cysteine crosslinking peptide GPQ-W (GCRDGPQG↓IWGQDRCG; ↓ denotes enzymatic cleavage site) or non-degradable crosslinking agent DTT (1,4-dithiothreitol; 3483-12-3, Sigma) was dissolved in HEPES at a density corresponding to 1:1 maleimide/cysteine ratio after accounting for maleimide groups reacted with adhesive peptide. For HIOs encapsulation, spheroids were embedded and expanded in Matrigel™ for up to 30 d. Resulting HIOs were dislodged from the Matrigel™ and resuspended at 5× final density (final density: 2-4 HIOs/hydrogel) in intestine growth medium³⁸ and kept on ice. For human intestinal spheroid encapsulation, spheroids were harvested immediately after differentiation and were resuspended at 5× final density (final density: 20-30 spheroids/hydrogel) in intestine growth medium and kept on ice. For HLOs encapsulation, these were dislodged from the Matrigel™ and resuspended at 5× final density (final density: 2-4 HLOs/hydrogel) in foregut growth medium^{27,28} and kept on ice. To form hydrogels, adhesive peptide-functionalized PEG-4MAL macromer, cells, and crosslinking peptide were polymerized for 20 min before addition of intestine growth medium. Matrigel™-generated hPSC-derived HIOs were generated and cultured as described previously^{13,38}. Passaging of HIOs cultured in PEG-4MAL hydrogels was performed similarly to tissue embedded in Matrigel™, as previously described^{27,38}. Briefly, HIOs were dislodged from the PEG-4MAL hydrogel, transferred to a sterile Petri dish, and manually cut into halves using a scalpel. HIO halves were resuspended at 5X final density (final density: 2-4 HIOs/hydrogel) in intestine growth medium³⁸ and mixed with hydrogel precursor solutions to form PEG-4MAL hydrogels. HIOs were passaged up to 3 times over the course of 3 weeks. Matrigel™-generated HIOs were passaged as described

previously^{13,38}. Sample size was established as at least 4 hydrogels per condition with the premise that an outcome present in 4 different hydrogels under a specific condition will reveal the population behavior submitted to this given condition.

A detailed protocol for generating the hydrogel and embedding HIOs can be found at the Protocol Exchange: DOI: 10.1038/protex.2017.098

Hydrogel characterization

The storage and loss moduli of hydrogels were assessed by dynamic oscillatory strain and frequency sweeps performed on a MCR 302 stress-controlled rheometer (Anton Paar) with a 9-mm diameter, 2° cone, and plate geometry. Oscillatory frequency sweeps were used to examine the storage and loss moduli ($\omega = 0.5\text{--}100 \text{ rad s}^{-1}$) at a strain of 2.3%.

Viability assay and quantification

PEG-4MAL gels were incubated in 2 μM Calcein-AM (live; Life Technologies), and 1 μM TOTO-3 iodide (dead; Life Technologies) in growth medium for 1 h. Samples were imaged using an Axiovert 35, Zeiss microscope. Quantification of viability was performed by calculating the percentage of the total projected area of a spheroid/organoid that stained positive for the live or dead stain using ImageJ (National Institute of Health, USA). The results are representative of three independent experiments performed with 6 PEG-4MAL/Matrigel™ gel samples per experimental group.

Inhibition of mediators of mechanotransduction

Inhibition of YAP, myosin II or Rho-associated kinase was performed using verteporfin (SML0534, Sigma), blebbistatin (203389, Calbiochem) and Y-27632 (688002, Calbiochem), respectively, by adding 10 or 30 μM to the intestine growth medium 20 min after spheroid encapsulation in hydrogel. Cell apoptosis/death was assessed 1 d after encapsulation using Annexin V/Dead Cell Apoptosis Kit (A13201, ThermoFisher). Samples were imaged using an Axiovert 35, Zeiss microscope. The results are representative of one experiment performed with 12 PEG-4MAL hydrogel samples per experimental group.

RT-qPCR

Total RNA from hESC day 0 spheroids or HIOs grown in PEG-4MAL hydrogels or Matrigel™ was extracted using the MagMax RNA isolation system and MagMax-96 total RNA isolation Kit (AM1830, ThermoFisher Scientific). cDNA was synthesized using the SuperScript VILO cDNA Synthesis Kit (11754-250, ThermoFisher Scientific). RT-qPCR was carried out using the QuantiTect SYBR Green PCR Kit (204145, Qiagen). Relative gene expression was plotted as Arbitrary Units using the formula: $[2^{-(\text{housekeeping gene Ct} - \text{gene of interest Ct})}] \times 10,000$. Primer sequences for RT-qPCR are provided in Supplementary Table 2.

Animal models

All animal studies were conducted following approved protocols established by University of Michigan's Institutional Animal Care and Use Committee (IACUC) in accordance with the U.S. Department of Agriculture (USDA) Animal and Plant Health Inspection Service

(APHIS) regulations and the National Institutes of Health (NIH) Office of Laboratory Animal Welfare (OLAW) regulations governing the use of vertebrate animals. Male (8 weeks old) NOD-scid IL2Rg-null (NSG) mice (Jackson Laboratory) were used for all experiments.

Kidney capsule implantation

Organoids were implanted under the kidney capsule of male NOD-scid IL2Rg-null (NSG) mice (Jackson Laboratory) as previously described (Watson et al., 2014 and Finkbeiner et al., 2015)²⁴. Briefly, mice were anesthetized using 2% isoflurane. The left flank was shaved and sterilized using chlorhexidine and isopropyl alcohol. A left flank incision was used to expose the kidney. HIOs were manually placed in a subcapsular pocket of the kidney using forceps. An intraperitoneal flush of Zosyn (100 mg/kg; Pfizer) was administered prior to closure in two layers. The mice were sacrificed and transplant retrieved after 12 weeks. The results are representative of one experiment performed with 3 mice per condition (one organoid implanted per kidney capsule). Sample size was established as 3 with the premise that an outcome present in 3 different animals under a specific condition will reveal the population behavior submitted to this given condition. No statistical method was used to predetermine sample size.

Colonic mucosal wound and HIO injections

NSG mice were anesthetized by intraperitoneal injection of a ketamine (100 mg/kg)/ xylazine (10 mg/kg) solution. A high-resolution miniaturized colonoscope system equipped with biopsy forceps (Coloview Veterinary Endoscope, Karl Storz) was used to biopsy-injure the colonic mucosa at 3–5 sites along the dorsal artery. Wound size averaged approximately 1 mm². HIO injection was performed on day 1 after wounding with the aid of a custom-made device comprising a 27-gauge needle (OD: 0.41 mm) connected to a small tube (Supplementary Fig. 6a). Endoscopic procedures were viewed with high-resolution (1,024 × 768 pixels) live video on a flat-panel color monitor. The results are representative of two independent experiments performed with 4 mice per condition (five colonic wounds/ injections per mouse) based on our previous experience with this model.

Wound closure quantification

Mice were anesthetized by intraperitoneal injection of a ketamine (10 g/L) xylazine (8 g/L) solution (10 µL/g body weight). To create mucosal injuries in the mouse colon and to monitor their regeneration, a high-resolution colonoscopy system was used. Each wound region was digitally photographed at day 1 and day 5, and wound areas were calculated using ImageJ (National Institute of Health, USA). In each experiment, 3 - 4 lesions per mouse were examined.

***In situ* hybridization (ISH)**

ISH for mouse *Lgr5* expression was performed on frozen sections fixed with 4% paraformaldehyde (PFA). Slides were permeabilized with proteinase K (3115887001, Sigma-Aldrich) for 30 min at 37°C, washed with Saline-Sodium Citrate buffer and then acetylated at room temperature for 10 min. Pre-hybridization step was performed for 1 h at

37°C in a humidified chamber. A DIG-labeled riboprobe diluted in hybridization buffer was incubated overnight at 68°C. The slides were then washed and blocked for 1 h at room temperature followed by incubation with DIG antibody (11093274910, Sigma-Aldrich) overnight at 4°C. The developer solution (11681451001, Roche) was incubated for 72 h until the *Lgr5+* cells became evident. ISH for *OLFM4* was performed using the RNAscope 2.5 HD manual assay with brown chromogenic detection (Advanced Cell Diagnostics, Inc.) per manufacturer's instructions. The human 20 base pair *OLFM4* probe was generated by Advanced Cell Diagnostics targeting 20 base pairs within 1111-2222 of *OLFM4* (gene accession NM_006418.4) and is commercially available. The results are representative of two independent experiments performed with 4 mice per condition (five colonic wounds/injections per mouse).

Statistics and reproducibility

All experiments were performed three or more times independently under similar conditions, except experiments shown in Fig. 6 and Supplementary Fig. 6, which were performed twice. Plots shown in Fig. 1b,d, 3a-c, 6e, and Supplementary Fig. 1c,d, 3, and 4 are for one of the experiments performed. Images shown in Fig. 4 and 5, and Supplementary Fig. 5 were performed once. Images shown in Fig. 2f,g, 3d,e, 4c,d, 5, 6c,d, and Supplementary Fig. 5b and 6b-d, are representative of at least 20 tissue slices that were stained and imaged for each specific marker per experimental group for each independent experiment. Images shown in Fig. 1a,c, 2a-e, 3a, and Supplementary Figs. 2, 3, and 5a, are representative of at least 3 images taken for each hydrogel per experimental group for each independent experiment. Images shown in Fig. 4a,b, and 6a,b,e, are representative of images taken for all organoids/dissected kidneys or each individual wound/injection per mouse for each independent experiment. All statistical analyses were performed using GraphPad Prism 6.0. Statistical significance was calculated by one-way analysis of variance (ANOVA) with Tukey's multiple comparisons test (Figs. 1b,d, 3a, and 6e), two-way repeated measures ANOVA (Fig. 3b,c), and unpaired t-test with Welch's correction (Supplementary Figs. 3b,c, and 4) as described in the figure legends. P-values of statistical significance are represented as **** $P < 0.0001$, *** $P < 0.001$, ** $P < 0.01$, * $P < 0.05$.

Data availability

Source data for Figs. 1b,d, 3a-c, and 6e, and Supplementary Fig. 1c,d, 3b,c, and 4 has been provided in Supplementary Table 1. Additional images for data in Fig. 4 and 5 are available at <https://figshare.com/s/41e24da45c18e768536e>. All other data supporting the findings of this study are available from the corresponding author on reasonable request.

Supplementary Material

Refer to Web version on PubMed Central for supplementary material.

Acknowledgments

This research was supported by the NIH (R01 AR062368, R01 AR062920 to A.J.G, R01 DK055679, R01 DK059888, DK055679, DK059888, and DK089763 to A.N.), and J.R.S. is supported by the Intestinal Stem Cell Consortium (U01DK103141), a collaborative research project funded by the National Diabetes and Digestive and Kidney Diseases (NIDDK) and the National Institute of Allergy and Infectious Diseases (NIAID), and by the

NIAID Novel, Alternative Model Systems for Enteric Diseases (NAMSED) consortium (U19AI116482), PHS Grant UL1TR000454 from the Clinical and Translational Science Award Program, and a seed grant from the Regenerative Engineering and Medicine Research Center between Emory University, Georgia Tech and the University of Georgia. R.C.A. is supported by a National Science Foundation Graduate Research Fellowship and M.Q. is supported by a fellowship from the Crohn's and Colitis Foundation of America (CCFA 326912).

References

1. Thomson JA, et al. Embryonic Stem Cell Lines Derived from Human Blastocysts. *Science*. 1998; 282:1145–1147. DOI: 10.1126/science.282.5391.1145 [PubMed: 9804556]
2. Takahashi K, et al. Induction of Pluripotent Stem Cells from Adult Human Fibroblasts by Defined Factors. *Cell*. 2007; 131:861–872. DOI: 10.1016/j.cell.2007.11.019 [PubMed: 18035408]
3. Takahashi K, Yamanaka S. A developmental framework for induced pluripotency. *Development*. 2015; 142:3274–3285. DOI: 10.1242/dev.114249 [PubMed: 26443632]
4. Fox IJ, et al. Stem cell therapy. Use of differentiated pluripotent stem cells as replacement therapy for treating disease. *Science*. 2014; 345:1247391. [PubMed: 25146295]
5. Robinton DA, Daley GQ. The promise of induced pluripotent stem cells in research and therapy. *Nature*. 2012; 481:295–305. DOI: 10.1038/nature10761 [PubMed: 22258608]
6. Huch M, et al. Long-term culture of genome-stable bipotent stem cells from adult human liver. *Cell*. 2015; 160:299–312. DOI: 10.1016/j.cell.2014.11.050 [PubMed: 25533785]
7. Yui S, et al. Functional engraftment of colon epithelium expanded in vitro from a single adult Lgr5(+) stem cell. *Nat Med*. 2012; 18:618–623. DOI: 10.1038/nm.2695 [PubMed: 22406745]
8. Fatehullah A, Tan SH, Barker N. Organoids as an in vitro model of human development and disease. *Nature cell biology*. 2016; 18:246–254. DOI: 10.1038/ncb3312 [PubMed: 26911908]
9. Clevers H. Modeling Development and Disease with Organoids. *Cell*. 2016; 165:1586–1597. DOI: 10.1016/j.cell.2016.05.082 [PubMed: 27315476]
10. Dekkers JF, et al. A functional CFTR assay using primary cystic fibrosis intestinal organoids. *Nat Med*. 2013; 19:939–945. DOI: 10.1038/nm.3201 [PubMed: 23727931]
11. Dekkers JF, et al. Characterizing responses to CFTR-modulating drugs using rectal organoids derived from subjects with cystic fibrosis. *Science Translational Medicine*. 2016; 8:344ra384–344ra384. DOI: 10.1126/scitranslmed.aad8278
12. Wells JM, Spence JR. How to make an intestine. *Development*. 2014; 141:752–760. DOI: 10.1242/dev.097386 [PubMed: 24496613]
13. Spence JR, et al. Directed differentiation of human pluripotent stem cells into intestinal tissue in vitro. *Nature*. 2011; 470:105–109. DOI: 10.1038/nature09691 [PubMed: 21151107]
14. Hughes CS, Postovit LM, Lajoie GA. Matrigel : A complex protein mixture required for optimal growth of cell culture. *PROTEOMICS*. 2010; 10:1886–1890. DOI: 10.1002/pmic.200900758 [PubMed: 20162561]
15. Gjorevski N, et al. Designer matrices for intestinal stem cell and organoid culture. *Nature*. 2016; 539:560–564. DOI: 10.1038/nature20168 [PubMed: 27851739]
16. Phelps EA, et al. Maleimide cross-linked bioactive PEG hydrogel exhibits improved reaction kinetics and cross-linking for cell encapsulation and in situ delivery. *Advanced materials*. 2012; 24:64–70. DOI: 10.1002/adma.201103574 [PubMed: 22174081]
17. Phelps EA, Headen DM, Taylor WR, Thule PM, Garcia AJ. Vasculogenic bio-synthetic hydrogel for enhancement of pancreatic islet engraftment and function in type 1 diabetes. *Biomaterials*. 2013; 34:4602–4611. DOI: 10.1016/j.biomaterials.2013.03.012 [PubMed: 23541111]
18. Enemchukwu NO, et al. Synthetic matrices reveal contributions of ECM biophysical and biochemical properties to epithelial morphogenesis. *The Journal of cell biology*. 2016; 212:113–124. DOI: 10.1083/jcb.201506055 [PubMed: 26711502]
19. Caiazzo M, et al. Defined three-dimensional microenvironments boost induction of pluripotency. *Nature materials*. 2016; 15:344–352. DOI: 10.1038/nmat4536 [PubMed: 26752655]
20. Wickström SA, Radovanac K, Fässler R. Genetic Analyses of Integrin Signaling. *Cold Spring Harbor Perspectives in Biology*. 2011; 3:a005116. [PubMed: 21421914]

21. Hoffman MP, et al. Laminin-1 and laminin-2 G-domain synthetic peptides bind syndecan-1 and are involved in acinar formation of a human submandibular gland cell line. *J Biol Chem.* 1998; 273:28633–28641. [PubMed: 9786856]
22. Emsley J, Knight CG, Farndale RW, Barnes MJ. Structure of the Integrin $\alpha 2\beta 1$ -binding Collagen Peptide. *Journal of Molecular Biology.* 2004; 335:1019–1028. DOI: 10.1016/j.jmb.2003.11.030 [PubMed: 14698296]
23. Kikkawa Y, et al. Laminin-111-derived peptides and cancer. *Cell adhesion & migration.* 2013; 7:150–256. DOI: 10.4161/cam.22827 [PubMed: 23263633]
24. Finkbeiner SR, et al. Transcriptome-wide Analysis Reveals Hallmarks of Human Intestine Development and Maturation In Vitro and In Vivo. *Stem Cell Reports.* 2015
25. Straight AF, et al. Dissecting Temporal and Spatial Control of Cytokinesis with a Myosin II Inhibitor. *Science.* 2003; 299:1743–1747. [PubMed: 12637748]
26. Uehata M, et al. Calcium sensitization of smooth muscle mediated by a Rho-associated protein kinase in hypertension. *Nature.* 1997; 389:990–994. [PubMed: 9353125]
27. McCracken KW, Howell JC, Wells JM, Spence JR. Generating human intestinal tissue from pluripotent stem cells in vitro. *Nat Protoc.* 2011; 6:1920–1928. DOI: 10.1038/nprot.2011.410 [PubMed: 22082986]
28. Dye BR, et al. A bioengineered niche promotes in vivo engraftment and maturation of pluripotent stem cell derived human lung organoids. *eLife.* 2016; 5:e19732. [PubMed: 27677847]
29. Dye BR, et al. In vitro generation of human pluripotent stem cell derived lung organoids. *eLife.* 2015; 4:e05098.
30. Finkbeiner SR, et al. Generation of tissue-engineered small intestine using embryonic stem cell-derived human intestinal organoids. *Biology Open.* 2015; 4:1462–1472. DOI: 10.1242/bio.013235 [PubMed: 26459240]
31. Gerbe F, Brulin B, Makrini L, Legraverend C, Jay P. DCAMKL-1 expression identifies Tuft cells rather than stem cells in the adult mouse intestinal epithelium. *Gastroenterology.* 2009; 137:2179–2180. author reply 2180–2171. DOI: 10.1053/j.gastro.2009.06.072 [PubMed: 19879217]
32. Leoni G, et al. Annexin A1-containing extracellular vesicles and polymeric nanoparticles promote epithelial wound repair. *The Journal of Clinical Investigation.* 2015; 125:1215–1227. DOI: 10.1172/JCI76693 [PubMed: 25664854]
33. Jang BG, et al. Distribution of intestinal stem cell markers in colorectal precancerous lesions. *Histopathology.* 2016; 68:567–577. DOI: 10.1111/his.12787 [PubMed: 26212207]
34. Besson D, et al. A Quantitative Proteomic Approach of the Different Stages of Colorectal Cancer Establishes OLFM4 as a New Nonmetastatic Tumor Marker. *Molecular & Cellular Proteomics : MCP.* 2011; 10:M111.009712.
35. van der Flier LG, Haegbarth A, Stange DE, van de Wetering M, Clevers H. OLFM4 Is a Robust Marker for Stem Cells in Human Intestine and Marks a Subset of Colorectal Cancer Cells. *Gastroenterology.* 2009; 137:15–17. doi: <http://dx.doi.org/10.1053/j.gastro.2009.05.035>. [PubMed: 19450592]
36. Barker N, et al. Identification of stem cells in small intestine and colon by marker gene Lgr5. *Nature.* 2007; 449:1003–1007. doi: http://www.nature.com/nature/journal/v449/n7165/supinfo/nature06196_S1.html. [PubMed: 17934449]
37. Kita-Matsuo H, et al. Lentiviral Vectors and Protocols for Creation of Stable hESC Lines for Fluorescent Tracking and Drug Resistance Selection of Cardiomyocytes. *PLoS ONE.* 2009; 4:e5046. [PubMed: 19352491]
38. Leslie JL, et al. Persistence and Toxin Production by *Clostridium difficile* within Human Intestinal Organoids Result in Disruption of Epithelial Paracellular Barrier Function. *Infection and Immunity.* 2015; 83:138–145. DOI: 10.1128/IAI.02561-14 [PubMed: 25312952]

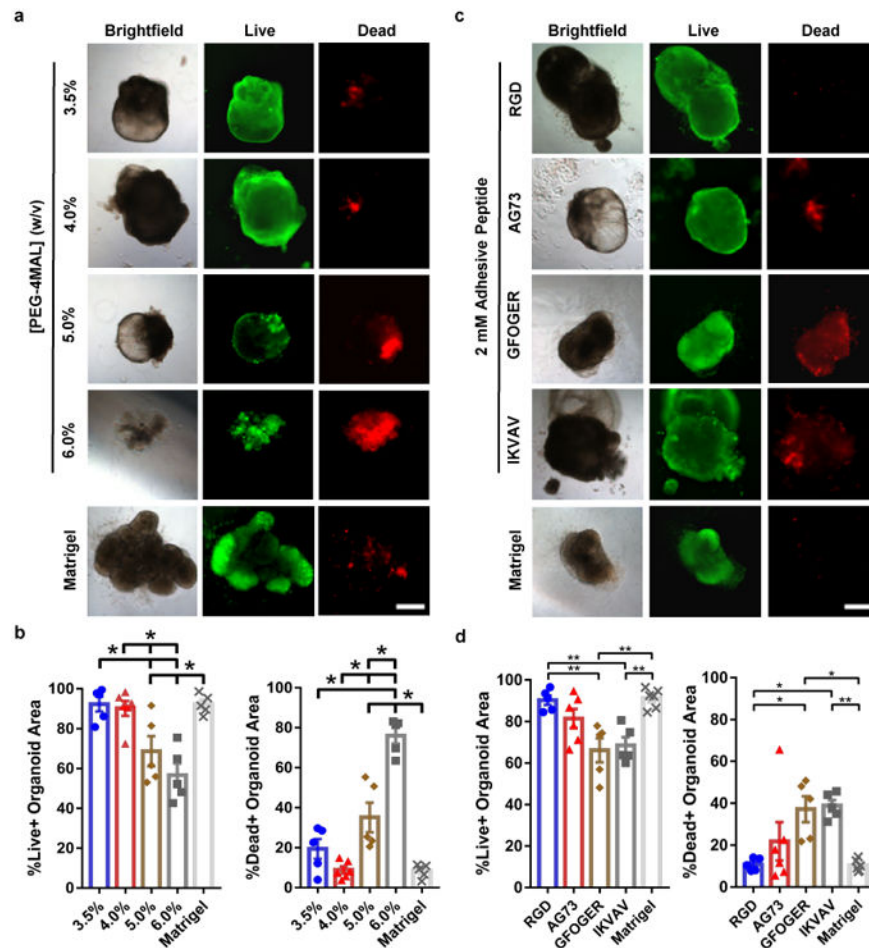


Figure 1. PEG-4MAL polymer density and adhesive ligand type control HIO viability
 (a) Transmitted light and fluorescence microscopy images of HIOs cultured in PEG-4MAL hydrogels of different polymer density or Matrigel™. HIO viability was assessed at 7 d after encapsulation. Bar, 500 μ m. (b) Percentage of total organoid area stained for live or dead (mean \pm SEM) after 7 d of encapsulation (n = 5 organoids analyzed for all groups, except n = 6 organoids analyzed for 4.0% group). (c) Transmitted light and fluorescence microscopy images of HIOs cultured in 4.0% PEG-4MAL hydrogels functionalized with different adhesive peptides or Matrigel™. HIO viability was assessed at 7 d after encapsulation. Bar, 500 μ m. (d) Percentage of total organoid area stained for live or dead (mean \pm SEM) after 7 d of encapsulation (n = 5 organoids analyzed for all groups, except n = 6 organoids analyzed for AG73 and Matrigel groups). (b,d) One-way ANOVA with Tukey's multiple comparisons test showed significant differences between (b) 4.0% PEG-4MAL or Matrigel™ and 5.0 or 6.0% PEG-4MAL, and between (d) PEG-4MAL-RGD or Matrigel™ and PEG-4MAL-GFOGER or -IKVAV. (* P < 0.05, ** P < 0.01, *** P < 0.001, **** P < 0.0001). (a-d) Three independent experiments were performed and data is presented for one of the experiments. Every independent experiment was performed with 6 gel samples per experimental group (PEG-4MAL, Matrigel™). Source data are available in Supplementary Table 1.

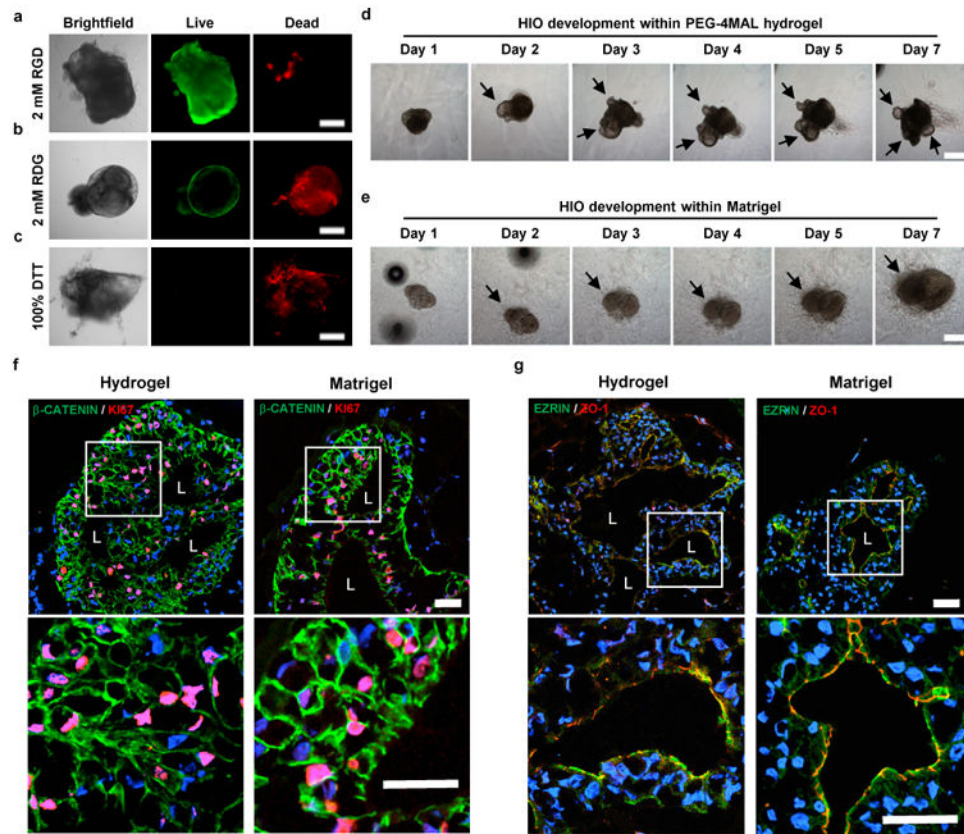


Figure 2. Engineered PEG-4MAL supports HIO development

(a) Transmitted light and fluorescence microscopy images of HIOs cultured in 4.0% PEG-4MAL hydrogels functionalized with (a) RGD, (b) inactive, scrambled RDG peptide, or (c) non-degradable crosslinker (DTT). HIO viability was assessed at 7 d after encapsulation. (d,e) Transmitted light microscopy images of MatrigelTM-generated HIOs cultured within (d) 4.0% PEG-4MAL-RGD hydrogel or (e) MatrigelTM over time. Bar, 500 μ m. (f,g) Fluorescence microscopy images of a HIO at 7 d after encapsulation in 4.0% PEG-4MAL-RGD hydrogel or MatrigelTM, and labeled for (f) β -CATENIN, proliferative cells (KI67), and (g) epithelial apical polarity (EZRIN) and tight junctions (ZO-1). DAPI, counterstain. “L” indicates HIO lumen. Bar, 100 μ m. (a-g) Three independent experiments were performed and data is presented for one of the experiments. Every experiment was performed with (a-c) 4, (f,g) 6 or (d,e) 12 gel samples per experimental group (PEG-4MAL, MatrigelTM).

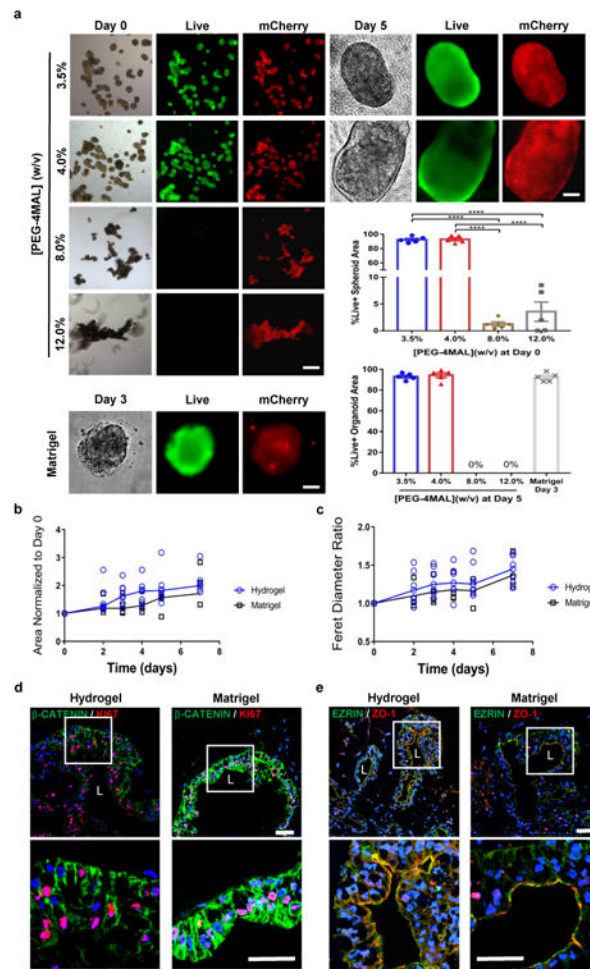


Figure 3. PEG-4MAL polymer density regulates HIO generation from intestinal spheroids in the absence of Matrigel

TM embedding. Transmitted light and fluorescence microscopy images of mCherry-spheroids cultured in PEG-4MAL hydrogels of different polymer density or MatrigelTM. Spheroids viability was assessed by Calcein-AM labeling at 2 h after encapsulation (day 0) and at day 5 for PEG-4MAL conditions, and at day 3 for MatrigelTM. Bar, 100 μ m. Viability is quantified as percentage of total spheroid or organoid area stained for live or dead (mean \pm SEM; $n = 5$ organoids analyzed per condition/time-point). One-way ANOVA with Tukey's multiple comparisons test showed significant differences between 3.5% or 4.0% PEG-4MAL and 8.0% or 12.0% PEG-4MAL at Day 0 (**** $P < 0.0001$). (b) HIO projected area and (c) Feret diameter normalized to Day 0 values at different time-points after encapsulation in 4.0% PEG-4MAL-RGD hydrogel (●) or MatrigelTM (■) ($n = 6$ organoids for PEG-4MAL and $n = 4$ organoids for MatrigelTM per time-point). Repeated measures two-way ANOVA showed no significant difference between matrix types ($P > 0.05$). Line represents the mean of the individual data points at each time-point. (d,e) Fluorescence microscopy images of a HIO at 21 d after encapsulation in 4.0% PEG-4MAL-RGD hydrogel or MatrigelTM and labeled for (d) β -CATENIN, proliferative cells (KI67), and (e) epithelial apical polarity (EZRIN) and tight junctions (ZO-1). DAPI, counterstain. "L" indicates HIO lumen. Bars, 100 μ m. Three independent experiments were performed and data is presented

for one of the experiments. Every experiment was performed with 6 gel samples per experimental group (PEG-4MAL, Matrigel™). Source data are available in Supplementary Table 1.

Author Manuscript

Author Manuscript

Author Manuscript

Author Manuscript

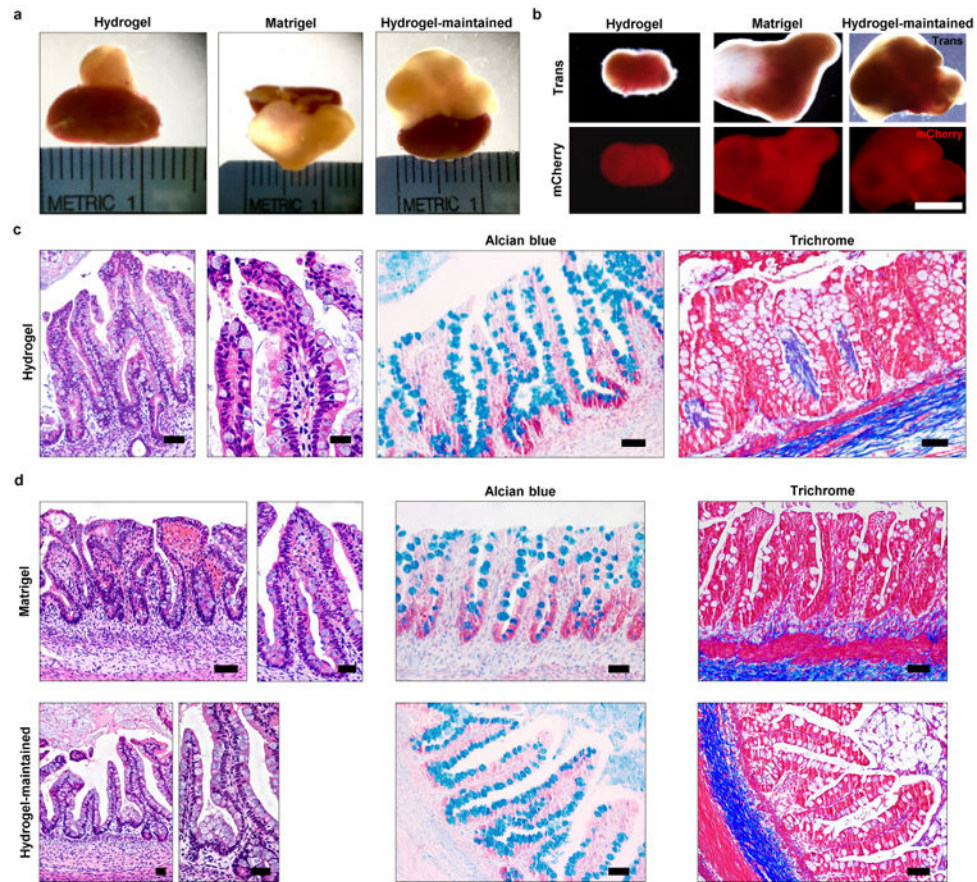


Figure 4. PEG-4MAL-generated HIOs develop a mature intestinal tissue structure *in vivo* (a) Micrographs of dissected kidneys containing HIOs generated within PEG-4MAL hydrogel, Matrigel™, or generated within Matrigel™ and maintained within PEG-4MAL (hydrogel-maintained). (b) Transmitted light and fluorescence microscopy (mCherry) images of harvested organoids. Bar, 0.5 cm. (c,d) H&E staining demonstrates mature human intestinal crypt-villus structure, and Alcian blue and trichrome staining reveal presence of differentiated goblet cells and organized collagen fibers. Bar, 100 μ m. One experiment was performed using 3 mice per experimental group.

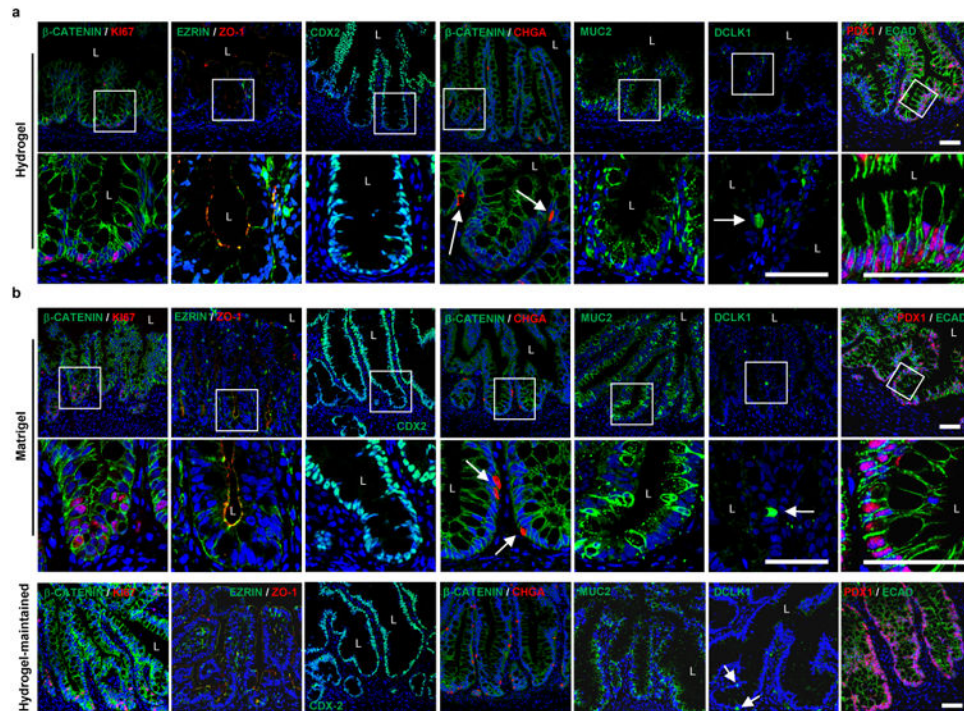


Figure 5. PEG-4MAL-generated HIOs differentiate into mature intestinal tissue *in vivo*
 (a,b) Fluorescence microscopy images of HIOs generated within (a) PEG-4MAL hydrogel, (b) Matrigel™, or generated within Matrigel™ and maintained within PEG-4MAL (hydrogel-maintained), and labeled for β -CATENIN, proliferative cells (KI67), epithelial apical polarity (EZRIN) and junctions (ZO-1 and ECAD), intestinal epithelial protein CDX2, enteroendocrine cells (CHGA), goblet cells (MUC2), tuft cells (DCLK1) and small intestinal marker (duodenum; PDX1). DAPI, counterstain. “L” indicates HIO lumen. White arrows show enteroendocrine cells or tuft cells. Bars, 50 μ m. One experiment was performed using 3 mice per experimental group.

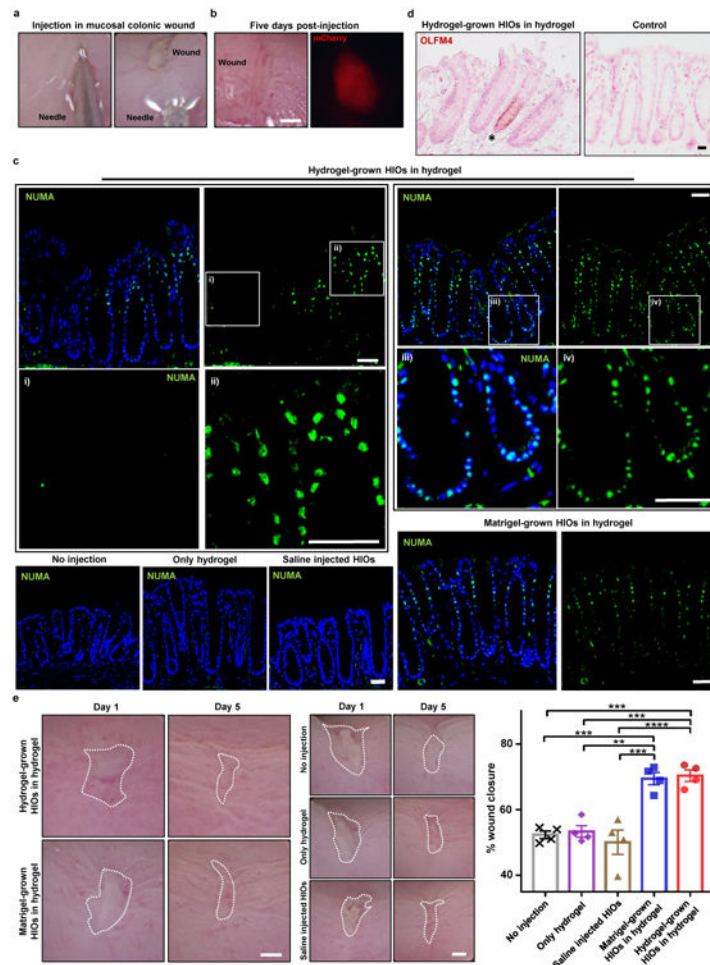


Figure 6. PEG-4MAL serves as an injectable delivery vehicle to promote HIO engraftment and wound closure

(a) PEG-4MAL-generated HIOs mixed with engineered hydrogel precursor solutions were injected underneath mechanically-induced mucosal wounds, as seen through the colonoscope camera. (b) Mechanically-induced mucosal wound and fluorescence imaging (mCherry) at the wound site at 5 d post-injection. Bar, 500 μ m. (c) Fluorescence microscopy images of murine colonic tissue at the wound site labeled for human cell nuclei (NUMA) at 4 weeks post-delivery. Left: Images from wound edge showing insets from i) adjacent host tissue and ii) wound. Right: Images from wound center showing insets at wound site. DAPI, counterstain. Bars, 100 μ m. (d) *In situ* hybridization, stained for human OLFM4+ cells. Bar, 50 μ m. (e) Images of mucosal wounds at 1 d (prior to injection) or 5 d post-injury in murine colon as seen through the colonoscope camera. Mucosal wound area at 5 d post-injury was normalized to day 1 (prior to injection) values (mean \pm SEM). Five colonic wounds per mouse were analyzed and averaged (n = 4 mice per condition). One-way ANOVA with Tukey's multiple comparisons test showed significant difference between hydrogel-grown HIOs in hydrogel (●) or MatrigelTM-grown HIOs in hydrogel (■) and saline-injected HIOs (▲), only hydrogel (♦), or no injection group (X) (** P < 0.01, *** P < 0.001, **** P < 0.0001). Bar, 500 μ m. Two independent experiments were performed and data is presented for one of the experiments. Experiments performed with 4 mice per experimental group (five

colonic wounds/injections per mouse; a-e). Source data are available in Supplementary Table 1.

Author Manuscript

Author Manuscript

Author Manuscript

Author Manuscript